Nature of electron states and symmetry breaking in quantum point contacts according to the local spin density approximation

2008 J. Phys.: Condens. Matter 20 164203

(http://iopscience.iop.org/0953-8984/20/16/164203)

IOP PUBLISHING JOURNAL OF PHYSICS: CONDENSED MATTER

J. Phys.: Condens. Matter **20** (2008) 164203 (8pp) doi:10.1088/0953-8984/20/16/164203

Nature of electron states and symmetry breaking in quantum point contacts according to the local spin density approximation

Karl-Fredrik Berggren and Irina I Yakimenko

IFM, Linköping University, S-58183 Linköping, Sweden

Received 9 October 2007, in final form 23 November 2007
Published 1 April 2008
Online at stacks.iop.org/JPhysCM/20/164203

Abstract

Electron states and local magnetization in quantum point contacts (QPCs) with different geometries and applied gate voltages are examined for a model GaAs/AlGaAs device. Using the local spin density approximation (LSDA) we recover ferromagnetic spatially split solutions in the pinch-off regime as well as antisymmetric solutions that occur with decreasing gate voltage. These kinds of spin states, which may appear in a repeated fashion in the few-electron regime, are precursors to an extended ferromagnetic state that may be associated with the 0.7 conductance anomaly. We briefly comment on some recent experiments indicating the presence of bound states (Yoon *et al* 2007 *Phys. Rev. Lett.* **99** 136805). We have not found any indication of such states but suggest that the accumulations of spin and charge at the two ends of a QPC and associated singlet and triplet states are relevant in this context.

1. Introduction

There is a rich physics and an elegant technology associated with gated modulation-doped semiconductor heterostructures like GaAs/AlGaAs. One attraction is the versatile high-mobility two-dimensional (2D) electron gas that resides at the semiconductor interface, a gas that may be shaped into different geometries by means of patterned metallic gates, for example, and whose density may be monitored by applied voltages. The structures in focus here are quantum point contacts (QPCs), which consist of narrow constrictions connected to surrounding 2D electron reservoirs. An electric current may be induced through the constriction when a voltage is applied over the two reservoirs that act as a source and a drain. As is well known, the conductance in high-mobility devices like these is quantized in steps of $2e^2/h$ [1, 2], which is a paradigm in modern mesoscopic physics. The quantized conductance is readily explained in terms of non-interacting electrons traversing a parabolic saddle potential, for example, with sub-band thresholds giving rise to the quantized conductance steps [3]. The phenomenon is quite robust, however, and occurs for smooth potential barriers in general.

In addition to the integer conduction steps, there is the remarkable $0.7(2e^2/h)$ conduction anomaly occurring below the lowest conduction plateau, as was first explored by Thomas and co-workers [4]. Because of its magnetic field dependence, the anomalous conductance behavior was immediately associated with spontaneous spin polarization. However, in contrast to the relatively straightforward one-electron physics for the integer steps, the true origin of the 0.7 anomaly is still disputed. There is an ever expanding literature on the effects of temperature, magnetic field, source–drain bias, device geometry etc, which is too rich to be summarized here. We therefore refer to some selected overviews [5–7] and references within.

Obviously the 0.7 feature results from electron interactions, but their exact role is, as indicated, not agreed on. Naturally there has been a number of different theoretical efforts, but here we limit our discussion to basically two main developments namely spontaneous spin-polarization and Kondo-like behaviour due to a bound state and single spin. In their pioneering work, Thomas *et al* [4] did emphasize the importance of spin splitting, which is a view that has been supported by numerous measurements for a variety of device geometries [5]. Therefore much theoretical work has been devoted to finding the mechanism behind with the Kohn–Sham (KS) local spin density approach (LSDA) as one of the essential computational tools [8]. The purpose of the present paper is to expand along this line, in particular to explore the pinch-off region in more detail. The KS approach, which incorporates the effects of

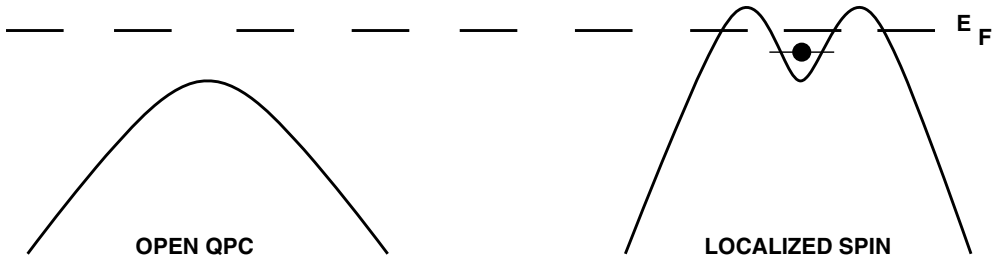

Figure 1. The left-hand panel shows schematically the transmission barrier for an open fully transmitting QPC. The right-hand panel illustrates a proposed scenario for the other extreme case, i.e. the region of pinch-off. Due to interactions, one anticipates a potential well occupied by a localized single spin at the center of the QPC [30–32]. The position of the Fermi energy, E_F, is shown by the broken horizontal line.

exchange and Coulomb interactions, willingly yields the local magnetization, as demonstrated for a single QPC and arrays of QPCs, long wires and coupled quantum dots [9–14][1]. The Kohn–Sham approach also predicts that spin polarization is accompanied by conductance anomalies in the range ∼0.5–0.7, depending on the device characteristics, as shown in, for example, [13–20] (see footnote 1). The spin-polarized two-band model also finds support in the phenomenological model by Reilly *et al* [21, 22], which was also recently used to explain the shot noise in a QPC [23] (see also [16, 24]). The '0.7 analogues' observed by Graham *et al* [25] due to Zeeman splitting at high magnetic fields may also be analyzed within the spin-relaxed Kohn–Sham formalism [26]. Exchange and correlation-driven spin polarization have also been shown to be of crucial importance for understanding magnetoconductance in wires [27].

The Kohn–Sham spin density formalism evidently predicts that local magnetization may occur spontaneously because of exchange and electron correlation effects. There is, however, a fundamental problem inherent in this approach, because it is in principle a zero-temperature theory. For this reason, it cannot reliably catch, for example, the anomalous temperature behavior [4, 28] and zero-bias anomaly [29] normally associated with the 0.7 conductance structure. To deal with these features, models have been introduced in which one assumes that there is a singly occupied bound state within the QPC itself and, because of this, the conductance is [28, 30, 31] thermally activated in a Kondo-like fashion [28, 30] and so on. The proposed appearance of a magnetic impurity at low electron densities is illustrated schematically in figure 1 (right-hand panel). This physical picture is also assumed by Yoon *et al* [32] to explain recent experiments for two QPCs in parallel and a certain resonant peak observed near pinch-off as one QPC is kept at a constant gate voltage while the voltage for other one is swept.

The Kondo-like model is successful in the sense that it accounts for thermal and magnetic behavior, finite voltage bias, etc. It appears, however, that there is also a fundamental problem with this model. Modeling with common realistic device parameters shows that bound states like the one in the right-hand panel of figure 1 do not exist within the QPCs. For this reason, one may question if the magnetic impurity model is generally valid (see also the comments in [33] on the existence of bound states).

In [13] it was noticed that local magnetization in a QPC may be reshaped quite drastically as one approaches the region of pinch-off. The polarized region that extends over the entire QPC at higher electron concentrations is then split in two parts that move to the two openings. Here we will explore this phenomenon in more detail using the Kohn–Sham spin density technique. Qualitatively, we find the rich scenario indicated in figure 2. Structures of this kind may be anticipated from [34–36], which examine the electron states in the interconnecting region between two few-electron dots. The nature of the electron states in a QPC near pinch-off is also investigated in [37] with a similar approach to that here. However, our emphasis on spin states, extension to re-entering states, and linear combinations of many-particle states into pure spin states, as in figure 3, etc is different.

Summing up, we find that questions about the nature of electron states and the possible formation of the magnetized state within QPCs remain most important for a proper understanding of QPC physics. In this paper we thus discuss the possibility of qualitatively different polarized states in QPCs and their dependence on the gate voltage. The model for numerical simulations and the Kohn–Sham spin density formalism are described in section 2. Results of the computations are presented in section 3, with an emphasis on the dependence of spin polarization on the length and width of a constriction as well as the gate voltage. Section 4 contains a summary and concluding remarks.

2. A model device

Our basic model device is the gated modulation-doped GaAs/AlGaAs heterostructure shown schematically in figure 4. Through appropriate combinations of materials, patterned gates, doping and applied gate voltages, the two-dimensional (2D) electron gas trapped at the AlGaAs/GaAs interface may be shaped and monitored in arbitrary ways by means of lithography and applied voltages. In the present case of a quantum point contact—the narrow channel connecting the two wide 2D reservoirs in figure 4—the electron density may be changed by an applied gate voltage, V_{sg}. For sufficiently strong negative voltages, the number of electrons becomes very

[1] For a discussion of the Bloch instability in narrow infinite rods and the role of electron correlation within different RPA-type approaches, see, for example, [7].

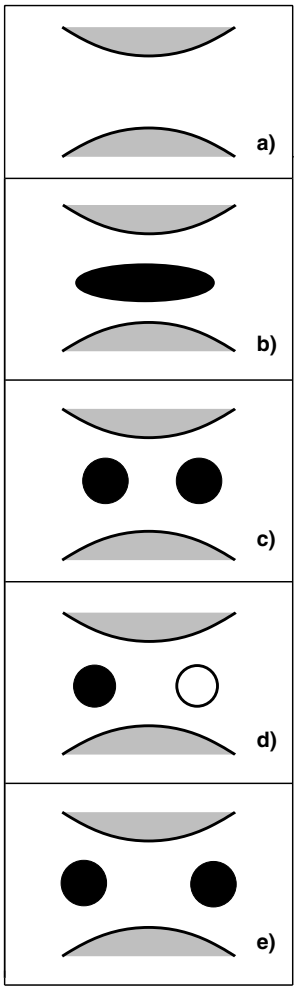

Figure 2. Progression of spin polarization (local magnetization) with decreasing conductance (gate voltage) towards pinch-off. Panel (a) illustrates a fully transmitting ballistic channel with $G = (2e^2/h)$. In this case there is no local magnetization within the QPC. As the conductance is lowered below the first plateau, spontaneous polarization driven by interactions sets in, as in (b). In this case the magnetization extends over the entire constriction. On a further decrease in the conductance, the magnetized region splits into two parts with spins in parallel, as in (c). On a further decrease in the gate voltage, a transition to a state with opposite spin directions may take place, as in (d). This may, in turn, give way to a new state with parallel spins, as in (c), but with increased spatial separation of the two regions. This kind of switching between spin states may occur repeatedly, as in (d), as electrons are continuously removed from the constriction by lowering the gate voltage towards pinch-off and below. The local pile up of spins is accompanied by charge accumulation.

low within the channel, which is eventually pinched-off. In this regime the role of electron interactions is evidently enhanced.

Transverse motions within the channel are quantized. The separation between associated sub-levels is small for wide channels. As a consequence, many channels are open and transmit currents. Therefore the channel is effectively 2D. On the other hand, in narrow channels only a small number of transverse modes remain occupied. The system then behaves as if it is quasi-one-dimensional (quasi-1D). In the quantum limit, which is in focus here, only the lowest mode is involved.

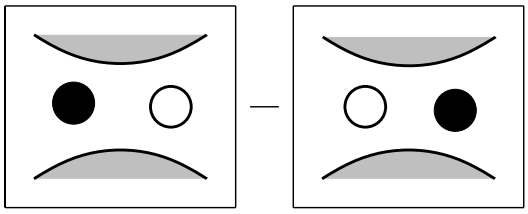

Figure 3. The antisymmetric state (d) in the previous figure is obviously degenerate with its mirror counterpart. Together, they may form an entangled singlet covalent type of state, illustrated schematically in this graph.

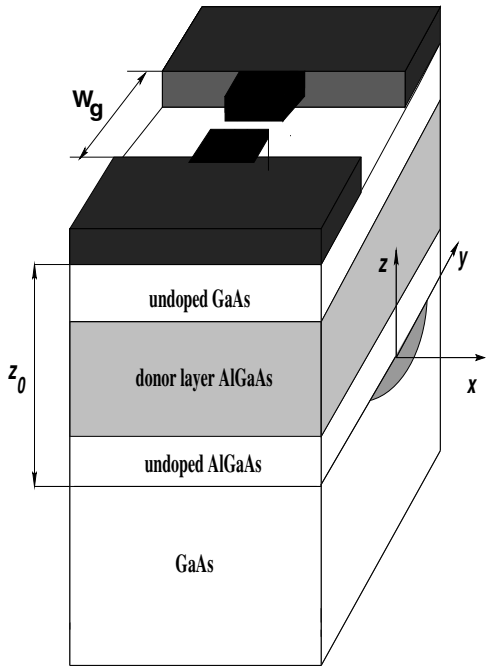

Figure 4. Schematic picture of the split gate device used in our modeling. The two-dimensional electron gas resides at the interface between the GaAs substrate and the spacer layer. The electron density is controlled by applied voltages V_g and V_{sg} between the gates (the split gate and the two fingers, respectively) and the substrate. Right and left ungated regions of lithographic width 400 nm serve as the source and drain, and the narrow middle section defines the QPC. Other parameters are: donor density is $\rho_d = 6 \times 10^{17}$ cm^{-3}, and the cap, donor and spacer layers are, respectively, 24, 36 and 10 nm thick, i.e. the same as in our previous studies, e.g. [13].

Below we trace the development of magnetized states in the interior of the QPC as the gate voltage V_{sg} is changed. As in our previous studies [13, 15, 18], the calculations are based on the Kohn–Sham equation for the 2D gas at the GaAs/AlGaAs interface,

$$\left[-\frac{\hbar^2}{2m^*}\nabla^2 + V^\sigma_{\rm eff}(x,y)\right]\psi^\sigma_{\rm k}(x,y) = E^\sigma_i\,\psi^\sigma_{\rm k}(x,y). \quad (1)$$

The effective potential in (1) consists of electrostatic confinement ($V_{\rm conf}$), Hartree ($V_{\rm H}$) and exchange–correlation ($V^\sigma_{\rm xc}$) terms:

$$V^\sigma_{\rm eff}(x,y) = V_{\rm conf}(x,y) + V_{\rm H}(x,y) + V^\sigma_{\rm xc}(x,y). \quad (2)$$

The electrostatic term contains four different contributions,

$$V_{\rm conf}(x, y) = -eV_{\rm g}(y) - eV_{\rm sg}(x, y) - eV_{\rm d} - eV_{\rm s}, \qquad (3)$$

where $V_{\rm g}$ is the potential from an infinite plane, held at a constant voltage, with a slit of width $W_{\rm g}$ (400 nm in our calculations), and $V_{\rm sg}$ is the potential from the central narrow split gate that defines the QPC. The rest of the terms correspond to the contributions from donors ($V_{\rm d}$) and surface states ($V_{\rm s}$) (see [13]). For $V_{\rm g}(y)$, an analytic expression is derived in [38]. To find $V_{\rm sg}$ we use numerical integration over the surface of the split gates. The Hartree term, $V_{\rm H}$, is also calculated numerically, including mirror charges from the ionized donors. For the exchange–correlation potential, $V_{\rm xc}$, we use the parameterization from [39]. Finally, in order to break the (spin) symmetry of the problem, we add a Zeeman term associated with a tiny magnetic field. The magnetic term is eventually switched off before self-consistency is reached in the numerical iteration process. To ensure that the final self-consistent solutions are not dependent on how the iterations are initiated, we have repeated the calculations, starting from weak random magnetic fields which are different for the two spin directions. As it turns out, the particular choice of trigger is not important for our final self-consistent results, which therefore represent ground-state solutions. More details of the model may be found, for example, in [13, 15, 18].

For convenience, we consider a periodic array of devices ordered along the x-axis in figure 4. In the calculations, the unit cell is then simply the split gate area. We solve the Kohn–Sham equation (1) self-consistently in the plane of the GaAs/AlGaAs interface by using periodic boundary conditions and by discretization on a grid. Specifically, we have studied QPCs of different lithographic length L (in the range 100–270 nm) and lithographic width W (in the range 10–80 nm). At each iterative step we find the eigenenergies, $E_{\rm k}^{\sigma}$, and the eigenstates, $\varphi_{\rm k}^{\sigma}$, for spin σ, and then calculate the electron density according to:

$$\rho^{\sigma}(x, y) = \sum_{E_{\rm k}^{\sigma} \leqslant \mu} \left|\varphi_k^{\sigma}(x, y)\right|^2. \qquad (4)$$

This expression corresponds to the ground-state equilibrium, i.e. there is no current induced by, for example, an applied source–drain voltage. In each step of the iterations we update the effective potential (2), whose value is used for the calculation of a new electron density. The iterative procedure is finished when consecutive electron densities become identical within a given tolerance.

The spin polarization of the system is calculated at the output of the iterative process as

$$p(x, y) = \rho^{\uparrow}(x, y) - \rho^{\downarrow}(x, y), \qquad (5)$$

i.e. the difference between the densities of ↑-spin and ↓-spin electrons. The periodic boundary conditions applied to a system imply the periodicity of the eigenfunctions,

$$\varphi_{\rm k}^{\sigma}(x + T, y) = \varphi_{\rm k}^{\sigma}(x, y)\mathrm{e}^{\mathrm{i}kT}, \qquad (6)$$

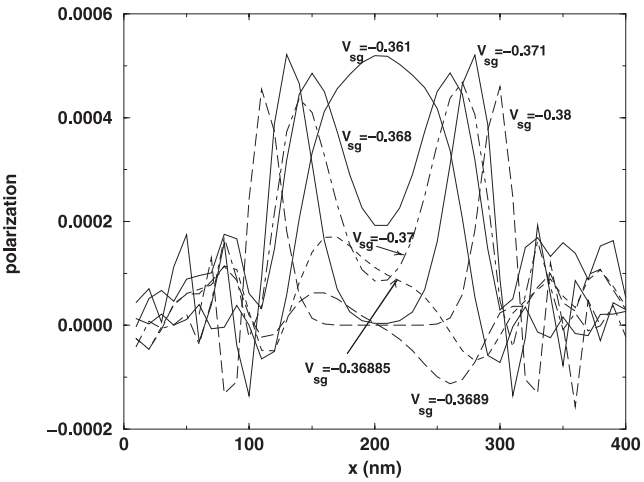

Figure 5. Local spin polarization in nm^{-2} ($p(x, y)$ in equation (5)) within a QPC of lithographic length 270 nm and width 10 nm for decreasing gate voltage $V_{\rm sg}$ (decreasing electron density in the QPC). The curves refer to the central symmetry line of the QPC ($y = 0$ in figure 4).

where T is the period in the x-direction (equal to 400 nm in our calculations) and k is the wavevector,

$$k = \frac{2\pi m}{MT}, \qquad (7)$$

where m is an integer belonging to the first Brillouin zone, $-M/2 < m \leqslant M/2$, where M is the number of unit cells (ten in our calculation). The period T is chosen here to be large enough so that neighboring QPCs do no interact. The computations are carried out for 0 K.

3. Results

As mentioned already, our focus is on the quantum limit with $G \leqslant 2e^2/h$ and cases with only a few electrons residing in the channel area, i.e. cases for which electron interactions are enhanced. The principal results for QPCs with different lithographic lengths and widths are summarized in figures 5–11.

The first appearance of local spin polarization/magnetization and its gradual development with decreasing gate voltages $V_{\rm sg}$/electron content are shown in figure 5 for a QPC with lithographic length $L = 270$ nm and width $W = 10$ nm. Initially, at higher voltages there is no polarization, as outlined schematically in figure 2(a). However, on lowering $V_{\rm sg}$, a pronounced spin polarization/magnetization extending over the entire QPC takes place for $V_{\rm sg} = -0.361$ V, once more as anticipated in figure 2(b). On a further decrease in the gate voltage, the polarized region gradually separates into two well-defined peaks located at the ends of the channel. At first the spins are aligned in parallel, as in figure 2(c) (the case $V_{\rm sg} = -0.368$ V). At $V_{\rm sg} = -0.368\,85$ V there is an onset towards an antisymmetric arrangement of spins. With a further small decrease in the gate voltage to $V_{\rm sg} = -0.3689$ V the spins at the two ends arrange themselves in an antisymmetric way, as anticipated in figure 2(d). The net polarization obviously

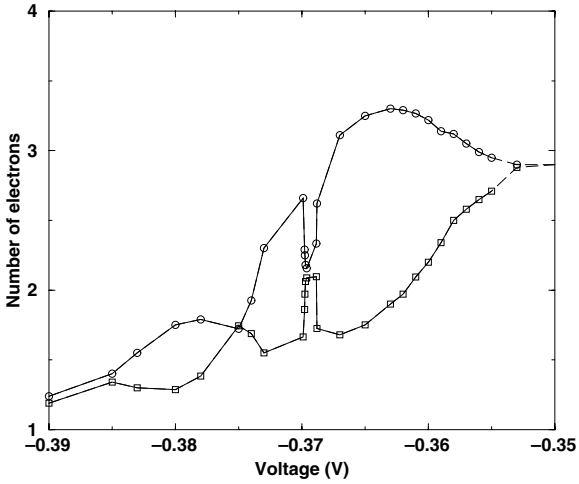

Figure 6. Number of up- and down-spin electrons versus gate voltage V_{sg} for a QPC with lithographic length 270 nm and width 10 nm. (○ and □ refer to up spins and down spins, respectively.) Polarization vanishes when the channel becomes fully open at $V_{sg} \sim -0.35$ V. The number of electrons is obtained by integrating $\rho^{\sigma}(x, y)$ over the QPC, as defined by lithography.

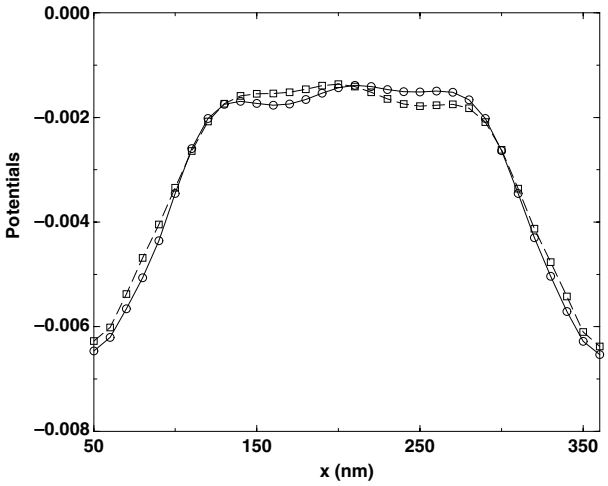

Figure 7. QPC potentials in eV for up- and down-spin electrons for a QPC with lithographic length 270 nm and width 10 nm at a gate voltage $V_{sg} = -0.3689$ V. The full drawn and dashed curves refer to spin-down and spin-up electrons, respectively. The curves refer to the middle of the QPC ($y = 0$ in figure 4). Here, E_F is set equal to zero.

vanishes in this case. At first sight, one may expect that this kind of spin arrangement and polarization inside the QPC would remain like this all the way towards pinch-off. However, a more detailed analysis of the pinch-off regime reveals another scenario. At $V_{sg} \leqslant -0.37$ V the polarization starts to grow, and new pronounced peaks with parallel polarization occur on both sides of the constriction, as shown for $V_{sg} = -0.371$ V in figure 2(d). The antisymmetric state re-enters briefly at $V_{sg} \leqslant -0.375$ V, but gives way to the spin parallel configuration on a further decrease in V_{sg}, as shown for $V_{sg} = -0.38$ V. In summary, the scenario outlined in figure 2 is confirmed by our simulations. The 'voltage windows' for the antisymmetric states are, however, quite narrow.

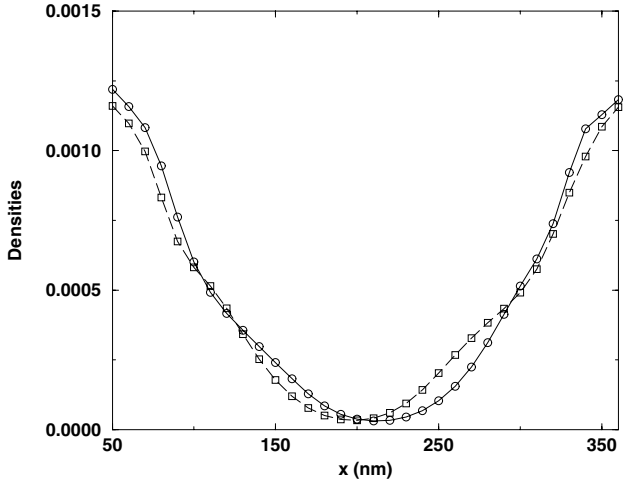

Figure 8. Densities in nm^{-2} for up- and down-spin electrons within a QPC with lithographic length 270 nm and width 10 nm at a gate voltage $V_{sg} = -0.3689$ V. (○ and □ refer to up spins and down spins, respectively.)

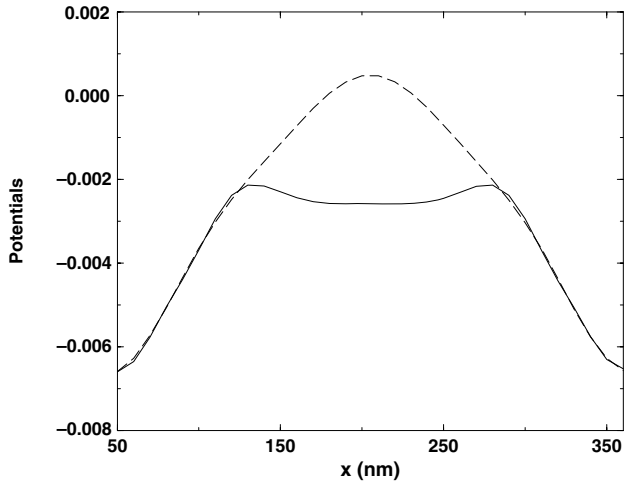

Figure 9. QPC potentials in eV for up- and down-spin electrons for a QPC of length 270 nm and width 10 nm at a gate voltage $V_{sg} = -0.361$ V (full and dashed curves, respectively). The two curves refer to the middle of the QPC ($y = 0$ in figure 4). Here E_F is set equal to zero.

The behavior of the number of up- and down-spin electrons as a function of V_{sg} are shown in figure 6 for the same case as above. The repeated appearance of antisymmetric configurations with decreasing gate voltage/number of electrons is clearly seen here. The antisymmetric and symmetry-breaking nature of these states is also clearly present in the spatial distributions of the potentials (figure 7) and electron densities (figure 8) for the two spin directions. For comparison, figure 9 shows the potentials at the gate voltage $V_{sg} = -0.361$ V, i.e. far from the antiferromagnetic domain. In this case the potential for spin-up electrons has a shallow minimum, but there is no sign for the formation of any bound state in the middle of the QPC, in accordance with previous findings [15, 18]. This result also holds for all other voltages referred to here.

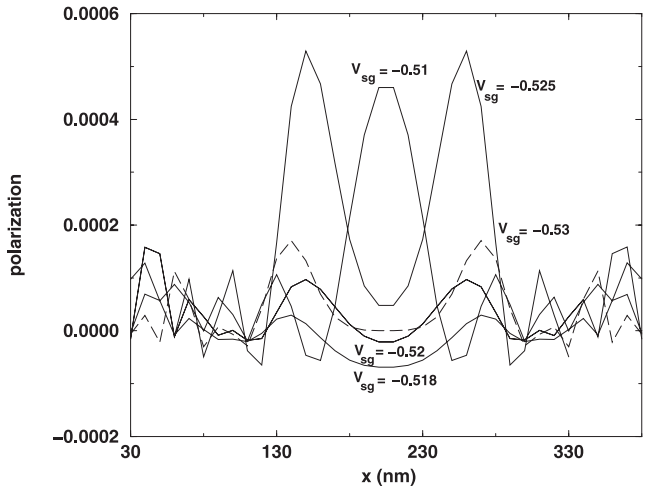

Figure 10. Local spin polarization in nm^{-2} within a QPC with lithographic length $L = 250$ nm and width $W = 80$ nm.

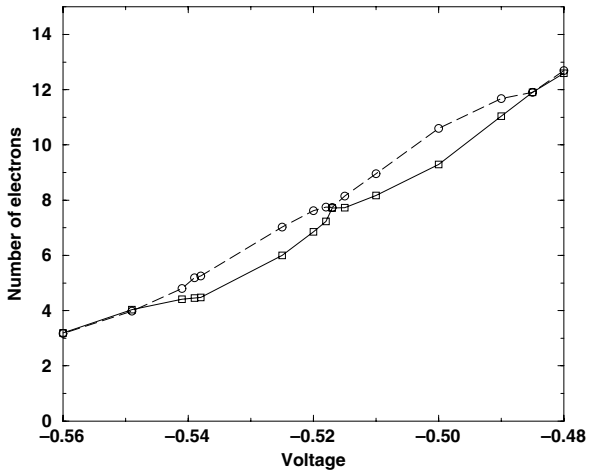

Figure 11. Number of up- (○) and down-spin (□) electrons within a QPC with lithographic length $L = 250$ nm and width $W = 80$ nm. The QPC is fully open ($G \sim 2e^2/h$) at $V_{\mathrm{sg}} \sim -0.48$ V and above.

We have also studied a QPC with the same lithographic width W as above, but with a shorter length L (200 nm). In this case the polarization is found to decrease four times in amplitude, and becomes almost indistinguishable from the polarization in the reservoirs. This confirms our earlier findings that only QPCs that are long enough possess appreciable spin-polarized states [18]. This also tells us that the geometry is very important for obtaining local magnetization.

The last series of our calculations is for a QPC of lithographic length $L = 250$ nm and width $W = 80$ nm. The results shown in figure 10 are similar to the above case, in the sense that the initially extended polarization (the case $V_{\mathrm{sg}} = -0.51$ V) splits into two peaks situated at the two ends of the QPC on lowering the voltage. As above, the spins are in parallel. That spin alignment then gives way to antiferromagnetic order (the cases $V_{\mathrm{sg}} = -0.518$ and -0.52 V in figure 10). Figure 10 also shows that there is an immediate return to parallel spin peaks on lowering V_{sg} slightly (the cases $V_{\mathrm{sg}} = -0.525$ and -0.53 V). Figure 11 shows how the number of up spins and down spins evolve with gate voltage. As in figure 6, the antiferromagnetic order exists only over a narrow voltage region. The resolution in gate voltage must therefore be very high to pin-point the antisymmetric (as in figure 5) or antiferromagnetic (as shown in figure 10) solutions. Near pinch-off the polarized regions are spatially well separated. Consequently, the interaction between them is very weak and the symmetric and antisymmetric solutions are very close in energy. In practice, they may even be degenerate [37].

4. Summary and concluding remarks

On the basis of the spin-relaxed Kohn–Sham equations (LSDA), we have investigated the nature of the electron states and the breaking of spatial and spin symmetries in a model split gate GaAs/AlGaAs device with realistic device parameters. We have focused on phenomena associated with the quantum limit, in particular on the conduction regime between a fully open channel and pinch-off ($G < 2e^2/h$). Throughout the simulations we have found it necessary to use a high resolution in gate voltage in order to uncover more subtle features in the electronic structure. As a consequence, the results in section 3 show that spin polarization/local magnetization within QPCs is generally far more complex than might be anticipated from a number of earlier investigations, for example [9, 13, 15–19, 21, 30]. For sufficiently long and electron-rich QPCs there is a variety of spin-polarized states that emerge as the gate voltage is swept towards the pinch-off regime. The most pronounced configuration corresponds to ferromagnetic spin ordering that extends over the entire constriction. This case is well known and is discussed in the references just cited. However, on lowering the electron content, the spatially extended polarization separates spontaneously into different polarized regions with either up- or down-spin orientations. These additional states, which thus occur near pinch-off and combine into overall antisymmetric (antiferromagnetic) or symmetric (ferromagnetic) arrangements of spins, peak at the two ends of the constriction. Depending on the specific geometry and electron content, there may be a sequence of crossovers between the two kinds of magnetized states, as there are many ways that spins may order into different spin multiplets. One scenario, although not undebated, associates the 0.7 anomaly with the onset of spin polarization. Thus, if there are more than one re-entries, as for example in figure 6, we should expect additional conduction anomalies at lower values than 0.7. As in [16, 18, 19], the conduction anomalies may be marked by a peak-like structure in conductance, as spins are rearranged while having different transmission coefficients. Features like these are, however, subtle and might be hard to observe experimentally. The voltage regions in which magnetic reordering occurs are quite narrow and the effects might be blurred by inhomogeneities and temperature [40].

We now turn to the nature of the electron states. Figures 5 and 10 show how spin polarization may peak at the two openings of a QPC. Accumulations of this kind might give

the impression of localization and bound states. However, we recall that there no bound states are found in the present modeling. All wavefunctions $\psi_k^\sigma(x, y)$ are extended and contribute collectively to the local build-up of spin polarization and charge [15]. In the same way, there is a pile-up of charge that accompanies these local magnetizations. Consequently, in the present LSDA picture there is no localization of magnetic moments and charge that derives from bound states embedded in a continuum, as speculated in figure 1 (right-hand panel). In this respect, we do not find support for models based on, for example, a Kondo-like mechanism [30, 32]. Rather than having a bound state in the middle of the QPC, we thus find, as the electron content is lowered, a collective build-up of spin and charge at the two QPC entries, as in figures 2(c) and (d).

The Kohn–Sham equations in equation (1) incorporate the effects of exchange and Coulomb interactions via an approximate potential $V_{xc}^\sigma(x, y)$. Basically, the KS equations refer to single electron states $\psi_k^\sigma(x, y)$, while the corresponding total wavefunction is a Slater determinant. Although the KS equations are conceptually and computationally very convenient, there is price to pay. Obviously, they cannot cope with multi-configurational situations. This is partly remedied by artificial symmetry breaking of the solutions $\psi_k^\sigma(x, y)$ as multi-configurational correlations become important. Typical examples are the antisymmetric states in figure 5. In this case the symmetry breaking of spatial symmetry leads to an overall incorrect symmetry of the total wavefunction. Nevertheless, the artificial symmetry breaking signals that certain correlations are important and are inherent in a properly symmetry-adapted total wavefunction and corresponding pair correlation functions $g_{\sigma,\sigma'}(r, r')$. Generally, symmetry may be restored from the KS solutions by combining equivalent states [10, 36]. For the antisymmetric states in figure 5 we would obviously think of pair-wise combinations of states, as suggested in figure 3, to form singlet states. In principle, such states are entangled. Higher-spin states such as triplets etc may, in principle, be constructed in similar ways. The restoration of proper symmetry states is, however, non-trivial, since we are dealing with a continuum of wavefunctions that contribute to the local pile-ups of spin and charge. So far, we have focused on the region close to pinch-off (cases (c) and (d) in figure 2). In the region (b), the electron content is higher and the ferromagnetic spin polarization extends over the entire QPC. Obviously, there are a multitude of possible spin states that become populated at finite temperatures and/or give rise to spin-wave-like scattering as a source–drain field is applied. We propose that these features, which have been overlooked so far, may be important for understanding the anomalous temperature dependence of the 0.7 structure.

Finally, we comment on a series of recent experiments concerning the interaction between two QPCs ([32] and references within). By sweeping the gate voltage of one QPC while keeping the voltage of the other one fixed near pinch-off, a resonant peak in the conductance was observed. This peak appears just near the pinch-off of the swept QPC and is taken as evidence for a single spin bound state in the center of a QPC, as in figure 1. As stressed here, we have not found evidence for bound states of this kind. Instead, we have argued that there is a rich structure of spin and charge pile-up at the two ends of a QPC. Close to pinch-off, one may recognize singlet and triplet states which might be associated with the resonance observed in [32].

Acknowledgment

Support from the Swedish Research Council is gratefully acknowledged. We are also grateful to M Pepper and J Bird for discussions and communications.

References

[1] Wharam D A, Thornton T J, Newbury R, Pepper M, Ritchie H and Jones G A C 1988 *J. Phys. C: Solid State Phys.* **21** L209
[2] van Wees B J, van Houten H, Beenakker C W J, Williamson J G, Kouwenhoven L P, van der Marel D, Foxton C T and Davies G J 1988 *Phys. Rev. Lett.* **60** 848
[3] Büttiker M 1990 *Phys. Rev.* B **41** 7906
[4] Thomas K J, Nicholls J T, Simmons M Y, Pepper M, Mace D R and Ritchie D A 1996 *Phys. Rev. Lett.* **77** 135
[5] Ferry D K, Goodnick S M and Bird J P 2008 *Transport in Nanostructures* 2nd edn Cambridge, at press
[6] Berggren K-F and Pepper M 2002 *Phys. World* **15** (10) 37–42
[7] Berggren K-F 2006 *Proc. Theor. Cond. Matter Workshop, (Ankara, Dec. 2005)*; *Turk. J. Phys.* **30** 197 http//journals.tubitak.gov.tr/physics
[8] Parr R G and Yang W 1989 *Density-Functional Theory of Atoms and Molecules* (New York: Oxford University Press)
[9] Wang C-K and Berggren K-F 1996 *Phys. Rev.* B **54** 14257
[10] Yakimenko I I, Bychkov A M and Berggren K-F 2001 *Phys. Rev.* B **63** 165309
[11] Berggren K-F, Yakimenko I I and Bychkov A M 2001 *Nanotechnology* **12** 529
[12] Heyman A, Yakimenko I I and Berggren K-F 2004 *Nanotechnology* **15** 143
[13] Berggren K-F and Yakimenko I I 2002 *Phys. Rev.* B **66** 085323
[14] Wang C-K and Berggren K-F 1998 *Phys. Rev.* B **57** 4552
[15] Starikov A A, Berggren K-F and Yakimenko I I 2003 *Phys. Rev.* B **67** 235319
[16] Havu P, Puska M, Nieminen R and Havu V 2004 *Phys. Rev.* B **70** 233308
[17] Ashok A, Akis R, Vasileska D and Ferry D K 2005 *Mol. Simul.* **31** 797
[18] Jaksch P, Yakimenko I I and Berggren K-F 2006 *Phys. Rev.* B **74** 235320
[19] Lassl A, Schlagheck P and Richter K 2007 *Phys. Rev.* B **75** 45346
[20] Bychkov A M and Stace T M 2007 *Nanotechnology* **18** 185403
[21] Reilly D J, Buehler T M, O'Brien J L, Hamilton A R, Dzurak A S, Clark R G, Kane B E, Pfeiffer L N and West K W 2002 *Phys. Rev. Lett.* **89** 246801
[22] Reilly D J 2005 *Phys. Rev.* B **72** 033309
[23] DiCarlo L, Yang Y, McClure D T, Reilly D J, Marcus C M, Pfeiffer L M and West K W 2006 *Phys. Rev. Lett.* **97** 36810
[24] Rokhinson L P, Pfeiffer L N and West K W 2006 *Phys. Rev. Lett.* **96** 156602
[25] Graham A C, Thomas K J, Pepper M, Cooper N R, Simmons M Y and Ritchie D A 2003 *Phys. Rev. Lett.* **91** 136404
[26] Berggren K-F, Jaksch P and Yakimenko I I 2005 *Phys. Rev.* B **71** 115303–1
[27] Zozoulenko I V and Ihnatsenka S 2008 Electron interaction and spin effects in quantum wires, quantum dots and quantum point contacts: first-principles mean-field approach *J. Phys.: Condens. Matter* **20** 164217

[28] Lindelof P E 2001 *Proc. SPIE* **4415** 77
[29] Cronenwett S M, Lynch H J, Goldhaber-Gordon D, Kouwenhoven L P, Marcus C M, Hirose K, Wingren N S and Umansky V 2002 *Phys. Rev. Lett.* **88** 226805
[30] Meir Y, Hirose K and Wingreen N S 2002 *Phys. Rev. Lett.* **89** 196802
[31] Hirose K, Meir Y and Wingreen N S 2003 *Phys. Rev. Lett.* **90** 026804
[32] Yoon Y, Mourokh L, Moriomoto T, Aoki N, Ochiai Y and Bird J P 2007 *Phys. Rev. Lett.* **99** 136805 and references within
[33] Ihnatsenka S and Zozoulenko I V 2007 *Phys. Rev.* B **76** 045338
[34] Wensauer A, Steffens O, Suhrke M and Rössler U 2000 *Phys. Rev.* B **62** 2605
[35] Kolehmainen J, Reinmann S M, Koskinen M and Manninen M 2000 *Eur. Phys. J.* B **13** 731
[36] Reinmann S M and Manninen M 2002 *Rev. Mod. Phys.* **74** 1283
[37] Rejec T and Meir Y 2006 *Nature* **442** 900
[38] Martorell J, Wu H and Sprung D W L 1994 *Phys. Rev.* B **50** 17298
[39] Tanatar B and Ceperley D M 1989 *Phys. Rev.* B **39** 5005
[40] Crook R, Prance J, Thomas K J, Farrer I, Chorley S J, Ritchie D A, Smith C G and Pepper M 2006 *Nature* **312** 1359